Available online at www.sciencedirect.com
ScienceDirect
Applied Mathematics and Computation xxx (2008) xxx–xxx
APPLIED MATHEMATICS AND COMPUTATION
www.elsevier.com/locate/amc

Approximate solution methods for one-dimensional solidification from an incoming fluid

S.L. Mitchell [a,*], T.G. Myers [b,1]

[a] MACSI, Department of Mathematics and Statistics, University of Limerick, Limerick, Ireland
[b] Department of Mathematics and Applied Mathematics, University of Cape Town, Rondebosch 7701, South Africa

Abstract

This paper concerns a one-dimensional model for solidification due to incoming supercooled liquid impacting on a substrate that is maintained at a fixed temperature. Using a boundary immobilisation method, and assuming that both the solid and liquid layers remain thin throughout the process, a second-order accurate perturbation expansion is determined. An alternative approximate solution, found using the heat balance integral method, is also described to analyse the problem, and the liquid height and temperatures in the solid and liquid are subsequently found for both approximate solutions. These are then compared with a numerical scheme which solves the full Stefan problem. The perturbation solution is shown to be more accurate, but the HBI method is simpler to implement and avoids complications that arise in the ordering of terms in the perturbation expansion as the difference between the substrate and melting temperature changes.

Keywords: Solidification; Heat balance integral; Boundary immobilisation; Thin film; Stefan problem

1. Introduction

The solidification of a molten material sprayed onto a substrate that is maintained at a temperature below the melting temperature has numerous natural and industrial applications. Perhaps the most common example being when atmospheric water freezes on a structure. This has been studied in the context of icing on power transmission and generating equipment, aircraft and seacraft, for example, see [6,12,13,16,17,20]. In an industrial setting solidification from a flowing liquid or a droplet spray is of interest in the casting of metals and spray forming, lava flows and hydrate build-up in oil pipelines [4,5,9]. In this paper, we focus on a particular situation, relevant to atmospheric icing, where the liquid spray is supercooled. Consequently, when it impacts on a surface that is below the solidification temperature the liquid immediately solidifies. If there is sufficient energy in the system then, once an insulating layer has built up, a liquid layer can form on the top of the solid layer. For ice accretion the initial layer is known as rime ice, the ice formed from a liquid layer is known as glaze ice.

* Corresponding author.
E-mail address: sarah.mitchell@ul.ie (S.L. Mitchell).
[1] Present address: Department of Mathematical Sciences, KAIST 373-1 Guseong-dong, Yuseong-gu, Daejeon 305-701, South Korea.

0096-3003/$ - see front matter © 2008 Elsevier Inc. All rights reserved.
doi:10.1016/j.amc.2008.02.031

One of the most challenging aspects of modelling ice accretion on structures is when there is a significant water layer [6,21]. This occurs when temperatures are relatively high and can lead to ice forming away from the main impact region. In a series of papers Myers and co-workers have developed a hierarchy of models starting with one-dimensional ice growth from an incoming supercooled water spray [14,18] to three-dimensional accretion and flow on a flat surface, which has then been extended to an arbitrary shaped surface [15–17]. In the current work we return to the basic problem, namely one-dimensional accretion, since an accurate model at this stage can be implemented at all subsequent stages of the hierarchy.

In the case of ice accretion on aircraft, the ice layer is never permitted to become large. Based on the assumption that both the ice and water layers remain thin throughout the process the analysis in [14–18] uses a leading order perturbation to determine the temperatures in the two layers. In the following analysis, we employ a boundary immobilisation method (BIM) which has been applied numerically to problems with a moving boundary by Crank [3] and more recently by Kutluay et al. [11]. This technique has also been used to obtain a perturbation solution to Stefan problems, see [2,10] and references therein. By changing the time variable to the ice thickness we can determine the perturbation solution up to second-order, and so improve on the accuracy of previous work. We also analyse the same problem using a heat balance integral (HBI) method, see [7,8]. Finally a numerical scheme is described, adapted from that of Brakel et al. [1], which is used to compare the accuracy of the perturbation and HBI solutions.

Although we are interested in general solidification problems we will confine our discussion to ice and water under aircraft icing conditions. Data for this situation are readily available, see [1,18]. We will also restrict our results to relatively high temperatures (typically down to around $-6\,^{\circ}\mathrm{C}$).

2. Governing equations

Consider a situation where a supercooled spray impacts on a surface. If the surface is below the solidification temperature then the initial droplets will freeze almost instantaneously. In mild temperatures, or when the solidified layer is sufficiently thick, a fluid layer may subsequently appear. In the following work we will focus on an ice and water system, although the model is equally applicable to other materials. The problem configuration is depicted in Fig. 1.

The temperatures in the ice and water are denoted by $\hat{T}(\hat{z},\hat{t})$ and $\hat{\theta}(\hat{z},\hat{t})$, respectively, and the thickness of each layer is $\hat{b}(\hat{t})$ and $\hat{h}(\hat{t})$. The problem is described by two heat equations:

$$\frac{\partial \hat{T}}{\partial \hat{t}} = \frac{k_{\mathrm{i}}}{\rho_{\mathrm{i}} c_{\mathrm{i}}} \frac{\partial^2 \hat{T}}{\partial \hat{z}^2}, \quad 0 \leqslant \hat{z} \leqslant \hat{b}, \tag{1}$$

$$\frac{\partial \hat{\theta}}{\partial \hat{t}} = \frac{k_{\mathrm{w}}}{\rho_{\mathrm{w}} c_{\mathrm{w}}} \frac{\partial^2 \hat{\theta}}{\partial \hat{z}^2}, \quad \hat{b} \leqslant \hat{z} \leqslant \hat{b} + \hat{h}, \tag{2}$$

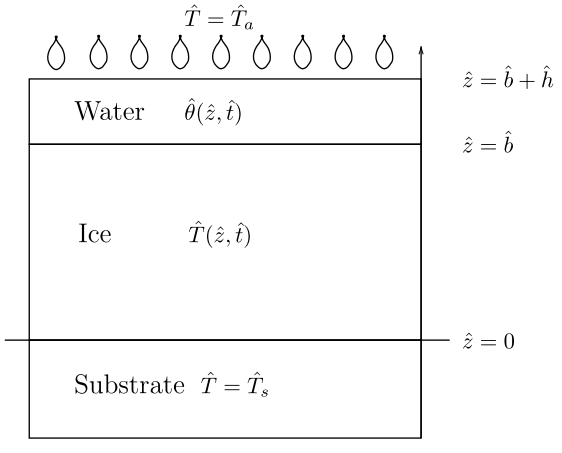

Fig. 1. Schematic of the 1D model problem.

Please cite this article in press as: S.L. Mitchell, T.G. Myers, Approximate solution methods for ..., Appl. Math. Comput. (2008), doi:10.1016/j.amc.2008.02.031

where k, ρ and c are the conductivity, density and specific heat capacity, respectively; a Stefan condition

$$\rho_i L_f \frac{d\hat{b}}{d\hat{t}} = k_i \frac{\partial \widehat{T}}{\partial \hat{z}} - k_w \frac{\partial \hat{\theta}}{\partial \hat{z}}, \quad \text{at } \hat{z} = \hat{b}(\hat{t}), \tag{3}$$

where L_f is the latent heat of freezing; and a mass balance,

$$\rho_i \frac{d\hat{b}}{d\hat{t}} + \rho_w \frac{d\hat{h}}{d\hat{t}} = \dot{m}, \tag{4}$$

where $\dot{m}$ is the rate at which mass enters from the spray.

We impose a fixed temperature boundary condition at the substrate $\hat{z} = 0$

$$\widehat{T}(0, \hat{t}) = \widehat{T}_s, \tag{5}$$

where $\widehat{T}_s$ is the substrate temperature. This is a reasonable approximation to the true state when the substrate is a good conductor with a relatively high thermal mass. A more general cooling condition is dealt with in [1,18], but we concentrate on this case here since it reduces the number of ice growth regimes and therefore allows us to focus on the solution methods. The extension to a cooling condition is straightforward. The remaining boundary conditions for (1)–(4) depend on the type of ice growth, either rime or glaze. To simplify the algebra we will restrict attention to the case, where $\widehat{T}_s$ is the same as the air temperature, $\widehat{T}_a$. This corresponds to the substrate being a good conductor with a region exposed to the air (as occurs with aircraft icing).

We now consider the rime and glaze ice growth separately.

- *Rime ice growth*: In this case there is no water layer present and so $\hat{h} \equiv 0$. We therefore only need to solve (1) over the domain $[0, \hat{b}]$, where $\hat{b} = \dot{m}t/\rho_i$ is determined from the integrated form of (4) with $\hat{b}(0) = 0$. An energy balance gives the boundary condition at the top of the ice layer $\hat{z} = \hat{b}$ (at the ice–air interface). We consider two different conditions, either a fixed or variable energy condition:

$$\text{(i)} \quad k_i \frac{\partial \widehat{T}}{\partial \hat{z}} = Q_i \quad \text{or} \quad \text{(ii)} \quad k_i \frac{\partial \widehat{T}}{\partial \hat{z}} = Q_i + q_l(\widehat{T}_s - \widehat{T}), \quad \text{at } \hat{z} = \hat{b}, \tag{6}$$

where the terms in Q_i may represent droplet kinetic energy, aerodynamic heating and latent heat, respectively, and q_l is composed of the droplet thermal energy, evaporation and convective heat transfer. The energy terms are discussed in detail in [1].The rime phase ends at time $\hat{t} = \hat{t}_w$, when the ice surface reaches the melting temperature $\widehat{T}(\hat{b}_w, \hat{t}_w) = \widehat{T}_f$ where $\hat{b}_w = \hat{b}(\hat{t}_w)$.
- *Glaze ice growth*: In this phase $\hat{h} > 0$ and we must solve (1)–(5) with the following boundary conditions. At the ice/water interface $\hat{z} = \hat{b}$, the temperatures are constant and equal to the melting temperature of the ice $\widehat{T}_f$, i.e.

$$\widehat{T}(\hat{b}, \hat{t}) = \widehat{T}_f = \hat{\theta}(\hat{b}, \hat{t}). \tag{7}$$

At the top of the water layer $\hat{z} = \hat{b} + \hat{h}$, similar conditions hold to those in (6), namely

$$\text{(i)} \quad k_w \frac{\partial \hat{\theta}}{\partial \hat{z}} = Q_w \quad \text{or} \quad \text{(ii)} \quad k_w \frac{\partial \hat{\theta}}{\partial \hat{z}} = Q_w + q_m(\widehat{T}_s - \hat{\theta}). \tag{8}$$

Provided $\dot{m}$ is constant, Eq. (4) integrates to

$$\rho_i(\hat{b} - \hat{b}_w) + \rho_w \hat{h} = \dot{m}(\hat{t} - \hat{t}_w), \tag{9}$$

using the initial condition $\hat{h}(\hat{t}_w) = 0$, and this allows us to eliminate $\hat{h}$ in subsequent calculations.

3. Non-dimensional analysis

The system is now non-dimensionalised in order to identify the dominant terms. We set

$$z = \frac{\hat{z}}{H}, \quad t = \frac{\hat{t}}{\tau}, \quad b = \frac{\hat{b}}{H}, \quad h = \frac{\hat{h}}{H}, \quad T = \frac{\widehat{T} - \widehat{T}_f}{\Delta T}, \quad \theta = \frac{\hat{\theta} - \widehat{T}_f}{\Delta T}, \tag{10}$$

Please cite this article in press as: S.L. Mitchell, T.G. Myers, Approximate solution methods for ..., Appl. Math. Comput. (2008), doi:10.1016/j.amc.2008.02.031

where $\Delta T = \widehat{T}_f - \widehat{T}_s$. Applying this scaling to the mass balance relation (4) gives

$$\frac{db}{dt} + \rho\frac{dh}{dt} = 1, \quad \rho = \frac{\rho_w}{\rho_i}, \tag{11}$$

provided we choose the timescale $\tau = \rho_i \mathscr{H}/\dot{m}$. The Stefan condition (3) is now

$$\frac{db}{dt} = \left[\frac{\partial T}{\partial z} - k\frac{\partial \theta}{\partial z}\right]_{z=b}, \quad k = \frac{k_w}{k_i}, \tag{12}$$

where the height-scale is

$$H = \frac{k_i \Delta T}{L_f \dot{m}}. \tag{13}$$

The choice of height and timescales is motivated by the fact that the mass balance and Stefan conditions obviously define the growth rates. The heat equations (1) and (2) therefore become

$$\epsilon_i \frac{\partial T}{\partial t} = \frac{\partial^2 T}{\partial z^2}, \quad \epsilon_i = \frac{c_i \mathscr{H} \dot{m}}{k_i}, \quad 0 \leqslant z \leqslant b, \tag{14}$$

$$\epsilon_w \frac{\partial \theta}{\partial t} = \frac{\partial^2 \theta}{\partial z^2}, \quad \epsilon_w = \rho\frac{c_w \mathscr{H} \dot{m}}{k_w}, \quad b \leqslant z \leqslant b + h. \tag{15}$$

The non-dimensional boundary condition (5) at the substrate–ice interface is now

$$T(0,t) = -1. \tag{16}$$

The rime boundary conditions (6) at the ice–air interface, $z = b$, are

$$\text{(i)} \quad \frac{\partial T}{\partial z} = P_i, \quad \text{or} \quad \text{(ii)} \quad \frac{\partial T}{\partial z} = P_i - p_i(1+T). \tag{17}$$

The glaze boundary conditions (7) and (8) become

$$T(b,t) = 0 = \theta(b,t), \tag{18}$$

and at $z = b + h$

$$\text{(i)} \quad \frac{\partial \theta}{\partial z} = P_w \quad \text{or} \quad \text{(ii)} \quad \frac{\partial \theta}{\partial z} = P_w - p_w(1+\theta), \tag{19}$$

where

$$P_i = \frac{Q_i \mathscr{H}}{k_i \Delta T}, \quad p_i = \frac{q_l \mathscr{H}}{k_i}, \quad P_w = \frac{Q_w \mathscr{H}}{k_w \Delta T}, \quad p_w = \frac{q_m \mathscr{H}}{k_w}. \tag{20}$$

The non-dimensional problem is now set up, so we move on to describe two approximate solutions, one found using a perturbation method and one found using a heat balance integral (HBI) method, and compare them to a numerical solution adapted from that given in [1].

4. Rime problem $0 < t < t_w$

In the rime period there is no water layer and so $b(t) = t$. Then from the previous section we have to solve

$$\frac{\partial^2 T}{\partial z^2} = \epsilon_i \frac{\partial T}{\partial t}, \quad 0 < z < b(t), \tag{21}$$

$$T(0,t) = -1, \quad \text{and} \quad \text{(i)} \quad \frac{\partial T}{\partial z} = P_i\Big|_{z=b} \quad \text{or} \quad \text{(ii)} \quad \frac{\partial T}{\partial z} = P_i - p_i(1+T)\Big|_{z=b}. \tag{22}$$

Please cite this article in press as: S.L. Mitchell, T.G. Myers, Approximate solution methods for ..., Appl. Math. Comput. (2008), doi:10.1016/j.amc.2008.02.031

4.1. The perturbation solution

The glaze problem, which is dealt with in the following section, is simplified by using b as the time variable (since $b(t)$ is monotonic it is valid to set $t = t(b)$). For the rime problem, $b = t$ and so this transformation is irrelevant. However, for consistency with the following section we will work with $t(b)$. We also use a co-ordinate system moving with the freezing boundary $y = z - b(t)$, otherwise known as the BIM [2,3,10,11], and denote $T(z, t) = S(y, b)$.

Under this co-ordinate change Eqs. (21) and (22) become

$$\frac{\partial^2 S}{\partial y^2} = \epsilon_i \left(\frac{\partial S}{\partial b} - \frac{\partial S}{\partial y} \right) \frac{db}{dt} = \epsilon_i \left(\frac{\partial S}{\partial b} - \frac{\partial S}{\partial y} \right), \quad -b < y < 0 \tag{23}$$

$$S(-b, b) = -1, \quad \text{and} \quad \text{(i)} \quad \frac{\partial S}{\partial y} = P_i \Big|_{y=0} \quad \text{or} \quad \text{(ii)} \quad \frac{\partial S}{\partial y} = P_i - p_i(1 + S) \Big|_{y=0}. \tag{24}$$

Provided ϵ_i is small, S may be expanded in powers of ϵ_i as

$$S = S_0 + \epsilon_i S_1 + \epsilon_i^2 S_2 + \cdots \tag{25}$$

and substituted into (23) and (24) to give

$$\frac{\partial^2 S_0}{\partial y^2} = 0, \quad \frac{\partial^2 S_k}{\partial y^2} = \frac{\partial S_{k-1}}{\partial b} - \frac{\partial S_{k-1}}{\partial y}, \tag{26}$$

for $k = 1, 2, \ldots,$ with $S_0(-b, b) = -1$, $S_k(-b, b) = 0$ and

$$\text{(i)} \quad \frac{\partial S_0}{\partial y} = P_i \Big|_{y=0}, \quad \frac{\partial S_k}{\partial y} = 0 \Big|_{y=0},$$

$$\text{(ii)} \quad \frac{\partial S_0}{\partial y} = P_i - p_i(1 + S_0) \Big|_{y=0}, \quad \frac{\partial S_k}{\partial y} = -p_i S_k \Big|_{y=0}.$$

Let us first consider the fixed energy condition (i) at the ice–air interface. The solution is given by

$$S_0 = P_i(y + b) - 1, \quad S_1 = S_2 = \cdots = 0, \tag{27}$$

and so $S(y, b) = P_i(y + b) - 1$. The rime period ends when $T(b_w, t_w) = 0$ or, equivalently, $S(0, b_w) = 0$. Hence the ice thickness and time at which the rime period ends occurs at $b_w = t_w = 1/P_i$. In terms of the physical parameters this is $t_w = L_f \dot{m}/Q_i$. It should be noted that back in the original co-ordinate system, the perturbation solution is $T(z, t) = P_i z - 1$ which is the exact solution in this case.

For the cooling condition (ii) at the ice–air interface, the leading order solution S_0 is

$$S_0(y, b) = A_0(b)(y + b) - 1, \quad A_0(b) = \frac{P_i}{1 + p_i b}. \tag{28}$$

In this case $S_k \neq 0$ for $k > 0$. To determine S_1 we must solve

$$\frac{\partial^2 S_1}{\partial y^2} = \frac{\partial S_0}{\partial b} - \frac{\partial S_0}{\partial y} = A_0'(b)(y + b), \quad S_1(-b, b) = 0, \quad \frac{\partial S_1}{\partial y} = -p_i S_1 \Big|_{y=0},$$

which leads to

$$S_1(y, b) = A_1(b)(y + b) + \frac{1}{6} A_0'(b)(y + b)[y^2 + 2b(y - b)], \quad A_1(b) = \frac{p_i A_0'(b) b^3}{3(1 + p_i b)}. \tag{29}$$

Also, the second-order solution S_2 is

$$S_2(y, b) = A_2(b)(y + b) + \frac{1}{6}(A_1'(b) - A_0'(b)b)(y + b)[y^2 + 2b(y - b)] + \frac{1}{120} A_0''(b)(y + b)[y^2 + 2b(y - 2b)]^2, \tag{30}$$

Please cite this article in press as: S.L. Mitchell, T.G. Myers, Approximate solution methods for ..., Appl. Math. Comput. (2008), doi:10.1016/j.amc.2008.02.031

where

$$A_2(b) = -\frac{2p_i A_0''(b)b^5}{15(1+p_i b)} + \frac{p_i(A_1'(b) - A_0'(b)b)b^3}{3(1+p_i b)}. \tag{31}$$

The time t_w when the rime period ends is then the solution of

$$S_0(0,t_w) + \epsilon_i S_1(0,t_w) + \epsilon_i^2 S_2(0,t_w) = 0,$$

which becomes

$$\begin{aligned} t_w &= \left\{ A_0(t_w) + \epsilon_i \left[A_1(t_w) - \frac{1}{3}A_0'(t_w)t_w^2 \right] + \epsilon_i^2 \left[A_2(t_w) - \frac{1}{3}(A_1'(t_w) - A_0'(t_w)t_w)t_w^2 + \frac{2}{15}A_0''(t_w)t_w^4 \right] \right\}^{-1} \\ &= \left\{ \frac{P_i t_w}{1+p_i t_w} + \frac{\epsilon_i p_i P_i t_w^3}{3(1+p_i t_w)^3} - \frac{\epsilon_i^2 p_i P_i t_w^4 (5 + p_i t_w + p_i^2 t_w^2)}{15(1+p_i t_w)^5} \right\}^{-1}. \end{aligned} \tag{32}$$

We can approximate t_w to the same level of accuracy as the temperature by taking

$$t_w = t_{w_0} + \epsilon_i t_{w_1} + \epsilon_i^2 t_{w_2} + \cdots = t_{w_0} - \frac{\epsilon_i p_i t_{w_0}^3}{3(1+p_i t_{w_0})} + \frac{\epsilon_i^2 p_i t_{w_0}^4 (15 + 18 p_i t_{w_0} + 8 p_i^2 t_{w_0}^2)}{45(1+p_i t_{w_0})^3}, \tag{33}$$

where

$$t_{w_0} = \frac{1}{P_i - p_i}. \tag{34}$$

The leading order term is singular when $P_i = p_i$. This reflects the possibility that a water layer may never appear and occurs when the incoming energy balances the heat loss. Using the expressions for P_i and p_i in (20) leads to the condition $\Delta T < Q_i/q_l$ (this may be seen as the requirement to have a positive temperature gradient in (6)). Since the fixed energy condition (24i) has no cooling, $p_i = 0$, and so provided $P_i > 0$ water will always appear in that case.

4.2. The quadratic HBI solution

We now consider the quadratic HBI solution of the systems (21) and (22). In [19] a cubic HBI solution, with no quadratic term, is used to approximate the temperature in a finite ice block. That choice was motivated by comparison with an exact solution, since the small z expansion gave this cubic form. Furthermore, a perturbation solution in the thin water layer also indicated the cubic profile was appropriate. In the current situation our perturbation solution includes a quadratic term at first-order, and so we stick with the standard quadratic HBI approximation. The solution method is now described for the boundary condition (ii) at the ice–air interface and then the solution for condition (i) follows directly by setting $p_i = 0$. In general, the quadratic heat balance integral method [7,8] involves assuming a solution of the form,

$$T(z,t) = a_0(t) + a_1(t)\left(1 - \frac{z}{b}\right) + a_2(t)\left(1 - \frac{z}{b}\right)^2, \tag{35}$$

where the coefficients $a_i(t)$ are unknown. We can immediately eliminate two of these by applying the boundary conditions in (22). Thus (35) reduces to

$$T(z,t) = -1 + \left(\frac{P_i b - (2 + p_i b)a_2}{1 + p_i b}\right)\frac{z}{b} + a_2\frac{z^2}{b^2}. \tag{36}$$

The remaining unknown coefficient $a_2(t)$ must now be determined by integrating the heat equations (2) from $z = 0$ to $z = b$,

$$\left.\frac{\partial T}{\partial z}\right|_{z=b} - \left.\frac{\partial T}{\partial z}\right|_{z=0} = \epsilon_i \left[\frac{\mathrm{d}}{\mathrm{d}t}\int_0^b T(z,t)\,\mathrm{d}z - \frac{\mathrm{d}b}{\mathrm{d}t}T(b(t),t) \right]. \tag{37}$$

Please cite this article in press as: S.L. Mitchell, T.G. Myers, Approximate solution methods for ..., Appl. Math. Comput. (2008), doi:10.1016/j.amc.2008.02.031

Then substituting T from (36) gives an ODE to solve for $a_2(t)$. At this stage Goodman and Shea [8] introduce the function $\psi(t) = \int_0^b T(z,t)\mathrm{d}z$, which has initial condition $\psi(0) = 0$, as there is not always an initial condition for the remaining unknown coefficient. In the present case we can determine that $a_2(0) = 0$ and so could solve for $a_2(t)$ directly. However, for the glaze problem it is more convenient to work with ψ, and the corresponding integral of θ, and so for consistency we also use this form here. Therefore (37) becomes

$$\frac{\mathrm{d}\psi}{\mathrm{d}t} = \left[\frac{2}{\epsilon_\mathrm{i} b} - \frac{1}{1+p_\mathrm{i} b}\right] a_2 + \frac{P_\mathrm{i} b}{1+p_\mathrm{i} b} - 1. \tag{38}$$

Before solving (38) we must eliminate $a_2(t)$ by re-writing it in terms of ψ as

$$a_2(t) = \frac{-6(1+p_\mathrm{i} b)(b+\psi(t)) + 3P_\mathrm{i} b^2}{b(4+p_\mathrm{i} b)}. \tag{39}$$

Since $b = t$ Eq. (38) is now a first-order differential equation for the single unknown $\psi(t)$. Once ψ is known we may determine $a_2(t)$ and hence $T(z, t)$ via Eq. (36).

Finally, the rime period ends at $t = b = t_\mathrm{w}$, where $T(t_\mathrm{w}, t_\mathrm{w}) = 0$. Using (36) this leads to

$$1 = \left(\frac{P_\mathrm{i} t_\mathrm{w} - (2+p_\mathrm{i} t_\mathrm{w}) a_2(t_\mathrm{w})}{1+p_\mathrm{i} t_\mathrm{w}}\right) + a_2(t_\mathrm{w}). \tag{40}$$

The solution for boundary condition (i) is simply found by setting $p_\mathrm{i} = 0$ in the above equations. In fact, for the fixed boundary condition, it can be shown that $a_2(t) = 0$ for all t. The simplest way to deduce this it to solve the ODE for $a_2(t)$ found from (37). The general solution, when $b = t$ and $p_\mathrm{i} = 0$, is given by $a_2(t) = C\sqrt{t}\mathrm{e}^{3/(\epsilon_\mathrm{i} t)}$ and we must set $C = 0$ to ensure a finite solution as $t \to 0$. Then the expression for T in (36) reduces to $T = -1 + P_\mathrm{i} z$ which is identical to the perturbation solution (and the exact solution).

4.3. The numerical solution

In this section we describe a semi-implicit finite difference scheme which is used to solve the systems (21) and (22), as developed for a related problem in [1].

The problem involves solving the heat equation in (21) with a moving boundary $z = b(t)$ and so the temperature profile T is calculated on a moving grid with a constant number of equally spaced mesh points. Since the height of the ice layer varies with time, the size of the mesh cell must be recalculated at each time step. This effect is dealt with by incorporating a convection term into the heat equation. Then the total derivative replaces the time derivative in the following way:

$$\frac{\mathrm{D}T}{\mathrm{D}t} = \frac{\partial T}{\partial t} + \frac{\partial T}{\partial z}\frac{\partial z}{\partial t} = \frac{1}{\epsilon_\mathrm{i}}\frac{\partial^2 T}{\partial z^2} + \frac{\partial T}{\partial z}\frac{\partial z}{\partial t}, \tag{41}$$

where $\frac{\partial z}{\partial t}$ is the speed of the moving grid and $\frac{\partial T}{\partial t}$ has been eliminated using (14). The discretised form of (41) is

$$\frac{T_j^{n+1} - T_j^n}{\Delta t} = \frac{1}{\epsilon_\mathrm{i}}\left(\frac{T_{j+1}^{n+1} - 2T_j^{n+1} + T_{j-1}^{n+1}}{{\Delta z_\mathrm{i}^{n+1}}^2}\right) + \frac{1}{2}\left[\frac{T_{j+1}^{n+1} - T_j^{n+1}}{\Delta z_\mathrm{i}^{n+1}}\left.\frac{\partial z_\mathrm{i}}{\partial t}\right|_{j+\frac{1}{2}} + \frac{T_j^{n+1} - T_{j-1}^{n+1}}{\Delta z_\mathrm{i}^{n+1}}\left.\frac{\partial z_\mathrm{i}}{\partial t}\right|_{j-\frac{1}{2}}\right], \tag{42}$$

which holds for $j = 1, \ldots, J_\mathrm{i} - 1$ and $n = 0, \ldots, N-1$. The subscript "i", denoting ice, is introduced here for convenience as it is necessary to distinguish between the meshes for ice and water in the numerical solution of the glaze problem, described in Section 5.3.

We write the discretisation in (42) as

$$\left[r_\mathrm{i} + \frac{v_\mathrm{i}}{2}\left.\frac{\partial z_\mathrm{i}}{\partial t}\right|_{j+\frac{1}{2}}\right] T_{j+1}^{n+1} - \left[1 + 2r_\mathrm{i} + \frac{v_\mathrm{i}}{2}\left(\left.\frac{\partial z_\mathrm{i}}{\partial t}\right|_{j+\frac{1}{2}} - \left.\frac{\partial z_\mathrm{i}}{\partial t}\right|_{j-\frac{1}{2}}\right)\right] T_j^{n+1} + \left[r_\mathrm{i} - \frac{v_\mathrm{i}}{2}\left.\frac{\partial z_\mathrm{i}}{\partial t}\right|_{j-\frac{1}{2}}\right] T_{j-1}^{n+1} = -T_j^n, \tag{43}$$

where

$$r_\mathrm{i} = \frac{\Delta t}{\epsilon_\mathrm{i}{\Delta z_\mathrm{i}^{n+1}}^2}, \quad v_\mathrm{i} = \frac{\Delta t}{\Delta z_\mathrm{i}^{n+1}}. \tag{44}$$

Please cite this article in press as: S.L. Mitchell, T.G. Myers, Approximate solution methods for ..., Appl. Math. Comput. (2008), doi:10.1016/j.amc.2008.02.031

Since $\frac{db}{dt} = 1$ in the rime period we have $b^{n+1} = b^n + \Delta t$ and so the parameters $\frac{\partial z_i}{\partial t}$ and Δz_i^{n+1} are evaluated as

$$\left.\frac{\partial z_i}{\partial t}\right|_j = \frac{j}{J_i}\frac{db}{dt} = \frac{j}{J_i}, \quad \Delta z_i^{n+1} = \frac{b^{n+1}}{\Delta t}. \tag{45}$$

We must now approximate the boundary conditions in (22). At the substrate–ice interface the condition $T(0, t) = -1$ is simply $T_0^{n+1} = -1$. To discretise condition (ii) at the ice–air interface we set $j = J_i$ in (42) and eliminate the first occurrence of $T_{J_i+1}^{n+1}$ using the discretised form,

$$\frac{T_{J_i+1}^{n+1} - T_{J_i-1}^{n+1}}{2\Delta z_i^{n+1}} = P_i - p_i(1 + T_{J_i}^{n+1}).$$

The second occurrence of $T_{J_i+1}^{n+1}$ is approximated slightly differently using

$$\frac{T_{J_i+1}^{n+1} - T_{J_i}^{n+1}}{\Delta z_i^{n+1}}\left.\frac{\partial z_i}{\partial t}\right|_{J_i+\frac{1}{2}} = [P_i - p_i(1 + T_{J_i}^{n+1})]\left.\frac{\partial z_i}{\partial t}\right|_{J_i} = P_i - p_i(1 + T_{J_i}^{n+1}),$$

since $\left.\frac{\partial z_i}{\partial t}\right|_{J_i} = 1$. Then the boundary condition (ii) becomes

$$\begin{aligned} &-\left[1 + 2r_i + 2p_i\Delta z_i^{n+1}r_i + p_i\Delta z_i^{n+1}\frac{v_i}{2} - \frac{v_i}{2}\left.\frac{\partial z_i}{\partial t}\right|_{J_i-\frac{1}{2}}\right]T_{J_i}^{n+1} + \left[2r_i - \frac{v_i}{2}\left.\frac{\partial z_i}{\partial t}\right|_{J_i-\frac{1}{2}}\right]T_{J_i-1}^{n+1} \\ &\quad = -T_{J_i}^n - 2(P_i - p_i)\Delta z_i^{n+1}r_i - (P_i - p_i)\Delta z_i^{n+1}\frac{v_i}{2} \end{aligned} \tag{46}$$

with (i) recovered by setting $p_i = 0$ in (46). This solution is valid whilst $T_{J_i}^{n+1} < 0$, and the time at which this condition is violated gives the numerical value of t_w.

5. Glaze ice growth $t > t_w$

During this phase the growth is governed by Eqs. (11), (12), (14), (15) subject to conditions (16), (18), (19). The initial condition $t = t_w$, $b = b_w$, $h = 0$ is determined from the solution in the rime stage.

5.1. The perturbation solution

With the change of variables $y = z - b(t)$ and $t = t(b)$, we write $T(z, t) = S(y, b)$, $\theta(z, t) = \phi(y, b)$. The thermal problem for the variable energy boundary condition (ii) may then be written as

$$\frac{\partial^2 S}{\partial y^2} = \epsilon_i\left(\frac{\partial S}{\partial b} - \frac{\partial S}{\partial y}\right)\frac{db}{dt}, \quad S(0, b) = 0, \quad S(-b, b) = 0, \tag{47}$$

$$\frac{\partial^2 \phi}{\partial y^2} = \epsilon_w\left(\frac{\partial \phi}{\partial b} - \frac{\partial \phi}{\partial y}\right)\frac{db}{dt}, \quad \phi(0, b) = 0, \quad \frac{\partial \phi}{\partial y} = P_w - p_w(1 + \phi)\Big|_{y=h} \tag{48}$$

with the problem for the simpler fixed energy boundary condition (i) the same but with $p_w = 0$. The Stefan condition (12) is now

$$\frac{db}{dt} = \left[\frac{\partial S}{\partial y} - k\frac{\partial \phi}{\partial y}\right]_{y=0} \tag{49}$$

and the mass balance (11) still holds which relates h to b. Note that we obviously require $\frac{dh}{dt} > 0$ and the solution below satisfies this at leading order for all $\Delta T \geqslant 0$.

Before finding a perturbation solution we need to think about the size of the small parameters, ϵ_i and ϵ_w, which are plotted against ΔT in Fig. 2. Clearly different terms dominate over different temperature regions, indicating that a variety of expansions are needed. For $\Delta T \in [0, 1]$ both ϵ_i and ϵ_w are very small, with $\epsilon_w \approx 10\epsilon_i$. In this range, a first-order expansion in ϵ_w should provide accurate results (with errors of around 0.4%). For $\Delta T \in [1, 5.5]$ we note $\epsilon_w^2 \sim \epsilon_i$ and an expansion to $\mathcal{O}(\epsilon_w^2)$ leads to errors typically less than 0.7%. In this case we may set $\epsilon_i = \beta\epsilon_w^2$. In the range $\Delta T \in [5.5, 8.5]$ we may set $\epsilon_i = \beta_1\epsilon_w^3$ and so on.

Please cite this article in press as: S.L. Mitchell, T.G. Myers, Approximate solution methods for ..., Appl. Math. Comput. (2008), doi:10.1016/j.amc.2008.02.031

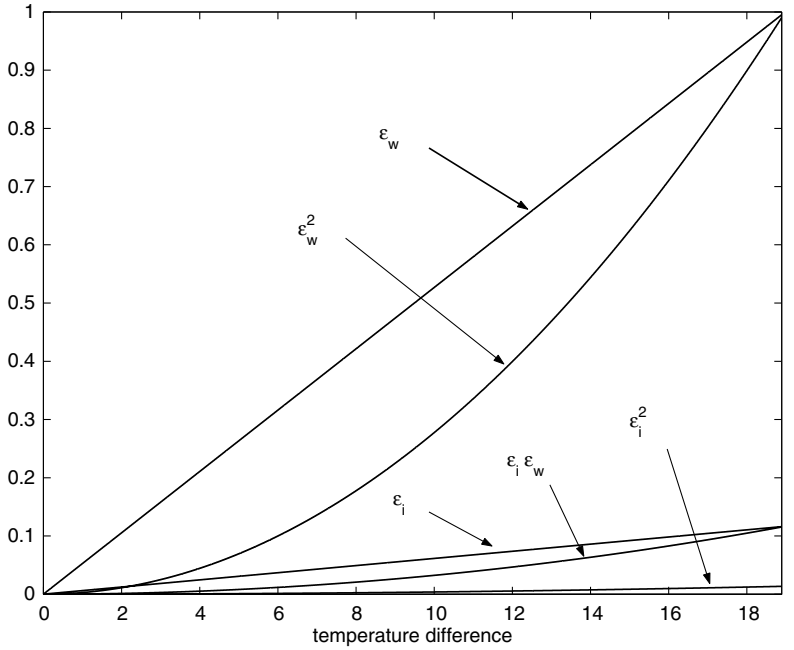

Fig. 2. Variation of ϵ_i, ϵ_w and second-order terms, plotted against Δt.

As discussed in Section 1 our primary interest is in relatively high temperatures, where a significant water layer appears. For this reason we will analyse $\Delta T \in [1, 5.5]$. The solution for $\Delta T < 1$ can be taken from the leading order terms of this solution. Expanding the temperatures as

$$S = S_0 + \epsilon_w^2 S_2 + \cdots, \quad \phi = \phi_0 + \epsilon_w \phi_1 + \epsilon_w^2 \phi_2 + \cdots$$

and substituting into (47) and (48) leads to

$$\frac{\partial^2 S_0}{\partial y^2} = 0, \quad S_0(0,b) = 0, \quad S_0(-b,b) = -1$$

$$\frac{\partial^2 S_2}{\partial y^2} = \beta\left(\frac{\partial S_0}{\partial b} - \frac{\partial S_0}{\partial y}\right)\left[\frac{\partial S_0}{\partial y} - k\frac{\partial \phi_0}{\partial y}\right]_{y=0}, \quad S_2(0,b) = 0, \quad S_2(-b,b) = 0$$

and

$$\frac{\partial^2 \phi_0}{\partial y^2} = 0, \quad \phi_0(0,b) = 0, \quad \frac{\partial \phi_0}{\partial y} = P_w - p_w(1+\phi_0)\Big|_{y=h},$$

$$\frac{\partial^2 \phi_1}{\partial y^2} = \left(\frac{\partial \phi_0}{\partial b} - \frac{\partial \phi_0}{\partial y}\right)\left[\frac{\partial S_0}{\partial y} - k\frac{\partial \phi_0}{\partial y}\right]_{y=0}, \quad \phi_1(0,b) = 0, \quad \frac{\partial \phi_1}{\partial y} = -p_w \phi_1\Big|_{y=h},$$

$$\frac{\partial^2 \phi_2}{\partial y^2} = \left(\frac{\partial \phi_0}{\partial b} - \frac{\partial \phi_0}{\partial y}\right)\left[-k\frac{\partial \phi_1}{\partial y}\right]_{y=0} + \left(\frac{\partial \phi_1}{\partial b} - \frac{\partial \phi_1}{\partial y}\right)\left[\frac{\partial S_0}{\partial y} - k\frac{\partial \phi_0}{\partial y}\right]_{y=0}, \quad \phi_2(0,b) = 0, \quad \frac{\partial \phi_2}{\partial y} = -p_w \phi_2\Big|_{y=h}.$$

For brevity, in this section we only give the results for boundary condition (i). The expansions for boundary condition (ii) are quoted in Appendix.

The leading order solutions with $p_w = 0$ are therefore

$$S_0 = A_0(b)y, \quad A_0(b) = \frac{1}{b}, \quad \text{and} \quad \phi_0 = B_0 y, \quad B_0 = P_w, \tag{50}$$

and the $\mathcal{O}(\epsilon_w)$ solution is given by

Please cite this article in press as: S.L. Mitchell, T.G. Myers, Approximate solution methods for ..., Appl. Math. Comput. (2008), doi:10.1016/j.amc.2008.02.031

$$\phi_1 = B_1(h)y - \frac{\lambda}{2}B_0 y^2, \quad B_1(b,h) = B_0\lambda h, \tag{51}$$

where

$$\lambda \equiv \lambda(b) = \left[\frac{\partial S_0}{\partial y} - k\frac{\partial \phi_0}{\partial y}\right]_{y=0} = A_0(b) - kB_0 = \frac{1}{b} - kP_{\mathrm{w}}. \tag{52}$$

Then the $\mathcal{O}(\epsilon_{\mathrm{w}}^2)$ solutions are

$$S_2 = A_2(b)y + \frac{\lambda\beta}{6}[A_0'(b)y^3 - 3A_0(b)y^2], \tag{53}$$

$$\phi_2 = B_2(b,h)y + \frac{1}{2}B_1(b,h)(kB_0 - \lambda)y^2 + \frac{\lambda}{6}(B_{1b} + B_0\lambda)y^3 - \frac{\lambda}{24}B_0\lambda_b y^4 \tag{54}$$

with

$$A_2(b) = \frac{\lambda\beta}{6}[A_0'(b)b^2 + 3A_0(b)b],$$

$$B_2(b,h) = -B_1(b,h)(kB_0 - \lambda)h - \frac{\lambda}{2}(B_{1b} + B_0\lambda)h^2 + \frac{\lambda}{6}B_0\lambda_b h^3,$$

where we have used B_{1b} to denote $\frac{\partial B_1}{\partial b}$. Substitution of expansions S and ϕ into the Stefan condition (49) gives

$$\begin{aligned}\frac{\mathrm{d}b}{\mathrm{d}t} &= \left[\frac{\partial S_0}{\partial y} + \epsilon_{\mathrm{w}}^2\frac{\partial S_2}{\partial y} - k\left\{\frac{\partial \phi_0}{\partial y} + \epsilon_{\mathrm{w}}\frac{\partial \phi_1}{\partial y} + \epsilon_{\mathrm{w}}^2\frac{\partial \phi_2}{\partial y}\right\}\right]_{y=0} \\ &= A_0(b) + \epsilon_{\mathrm{w}}^2 A_2(b) - k\{B_0 + \epsilon_{\mathrm{w}}B_1(h) + \epsilon_{\mathrm{w}}^2 B_2(h)\},\end{aligned} \tag{55}$$

subject to the initial condition $b = b_{\mathrm{w}}$ at $t = t_{\mathrm{w}} = b_{\mathrm{w}}$. The substitution $h = (t-b)/\rho$ reduces Eq. (55) to a first-order ordinary differential equation for b. Note that the expression for ϕ_2 contains the term $h_b = (t_b - 1)/\rho$, where t_b may be replaced using $t_b = 1/\lambda$. This is a leading order approximation which is sufficient here since h_b only appears at second-order. However, for the boundary condition (ii) this quantity appears at first-order and so we must expand t_b as $t_{b,0} + \epsilon_{\mathrm{w}}t_{b,1}$. This is discussed in more detail in Appendix.

Once Eq. (55) is solved, we can calculate $h(t)$ and consequently the temperature profiles in the two layers.

5.2. The quadratic HBI solution

The method for determining the quadratic HBI solution for glaze growth is similar to that discussed in Section 4.2. We briefly describe the solution method for the boundary condition (ii) at the water–air interface and then the solution for condition (i) follows directly by setting $p_{\mathrm{w}} = 0$. The solution for T is again of the form (35) and similarly for θ we assume

$$\theta(z,t) = c_0(t) + c_1(t)\left(\frac{b+h-z}{h}\right) + c_2(t)\left(\frac{b+h-z}{h}\right)^2, \tag{56}$$

where the coefficients $a_{\mathrm{i}}(t)$ and $c_{\mathrm{i}}(t)$ are unknown. Note that we have divided by h in (56) as this is the width of the water region, and it simplifies the algebra when dealing with the boundary condition at $z = b + h$.

We can immediately eliminate four of the coefficients by applying the boundary conditions in (16), (18), (19ii). Thus T in (35) is simply

$$T(z,t) = -1 + (1-a_2)\frac{z}{b} + a_2\frac{z^2}{b^2}, \tag{57}$$

and θ in (56) becomes

$$\theta(z,t) = \frac{(P_{\mathrm{w}} - p_{\mathrm{w}})h - c_2}{1 + p_{\mathrm{w}}h} - \frac{(P_{\mathrm{w}} - p_{\mathrm{w}})h + c_2 p_{\mathrm{w}}h}{1 + p_{\mathrm{w}}h}\left(\frac{b+h-z}{h}\right) + c_2\left(\frac{b+h-z}{h}\right)^2. \tag{58}$$

Please cite this article in press as: S.L. Mitchell, T.G. Myers, Approximate solution methods for ..., Appl. Math. Comput. (2008), doi:10.1016/j.amc.2008.02.031

The remaining unknown coefficients $a_2(t)$ and $c_2(t)$ must now be determined by integrating the heat equation (14) from $z = 0$ to $z = b$ and (15) from $z = b$ to $z = b + h$. Hence

$$\frac{\mathrm{d}\psi}{\mathrm{d}t} = \frac{2a_2}{\epsilon_\mathrm{i} b}, \quad \frac{\mathrm{d}\chi}{\mathrm{d}t} = \frac{2c_2}{\epsilon_\mathrm{w} h} + \left(\frac{\mathrm{d}b}{\mathrm{d}t} + \frac{\mathrm{d}h}{\mathrm{d}t}\right)\left[\frac{(P_\mathrm{w} - p_\mathrm{w})h - c_2}{1 + p_\mathrm{w} h}\right], \tag{59}$$

where

$$\psi(t) = \int_0^b T\,\mathrm{d}z, \quad \chi(t) = \int_b^{b+h} \theta(z,t)\,\mathrm{d}z. \tag{60}$$

As discussed for the HBI solution in the rime region in Section 4.2, we find it convenient to use these integrals as it is not clear how to choose initial conditions for a_2 and c_2 and the resulting ODEs are more complicated. Using these expressions we can eliminate a_2 and c_2 from (59) by re-writing them in terms of ψ and χ, i.e.

$$a_2 = -3 - \frac{6\psi}{b}, \quad c_2 = \frac{3(P_\mathrm{w} - p_\mathrm{w})h}{4 + p_\mathrm{w} h} - \frac{6(1 + p_\mathrm{w} h)\chi}{h(4 + p_\mathrm{w} h)}. \tag{61}$$

The pair of first-order differential equations in (59) must be coupled with (11) and (12) to give a system of four equations for the four unknowns ψ, χ, b and h. However, h can immediately be eliminated by writing it in terms of b as $h = (t - b)/\rho$. The Stefan condition (12) becomes

$$\frac{\mathrm{d}b}{\mathrm{d}t} = \frac{1 + a_2}{b} - k\left[\frac{(P_\mathrm{w} - p_\mathrm{w})h - (2 + p_\mathrm{w} h)c_2}{h(1 + p_\mathrm{w} h)}\right] \tag{62}$$

and the system (59) and (62) can be solved subject to initial conditions $\psi(t_\mathrm{w}) = \psi_\mathrm{w}$ (found from the rime solution), $\chi(t_\mathrm{w}) = 0$ and $b(t_\mathrm{w}) = t_\mathrm{w}$.

Again note that condition (i) at the water–air interface is recovered by setting $p_\mathrm{w} = 0$ in the above analysis.

5.3. The numerical solution

We now explain how to extend the semi-implicit finite difference scheme described in Section 4.3 to include the water layer which develops in the glaze period. The rime model is run until T exceeds zero. The final value profile in the rime region which satisfies $T_{J_\mathrm{i}}^{n+1} < 0$ is the initial condition for the glaze solution. At the top of the ice layer the boundary condition (17) is replaced by (18) and so $\theta_0^{n+1} = 0$.

The ice and water growth thicknesses b and h are determined by

$$b^{n+1} = b^n + \Delta t b_t^n, \quad h^{n+1} = h^n + \Delta t h_t^n, \tag{63}$$

for $n = 0, \ldots, N - 1$, where b_t^n and h_t^n are found by discretising (11) and (12) as follows: the former is simply $h_t^n = (1 - b_t^n)/\rho$ and then

$$b_t^n = \frac{3T_{J_\mathrm{i}}^n - 4T_{J_\mathrm{i}-1}^n + T_{J_\mathrm{i}-2}^n}{2\Delta z_\mathrm{i}^n} - k\left(\frac{-3\theta_0^n + 4\theta_1^n - \theta_2^n}{2\Delta z_\mathrm{w}^n}\right). \tag{64}$$

Note that to determine b^1 in (63) we need to use the final profile in the rime region which satisfies $T_{J_\mathrm{i}}^{n+1} < 0$. This gives $T_{J_\mathrm{i}}^0$, $T_{J_\mathrm{i}-1}^0$ and $T_{J_\mathrm{i}-2}^0$ in b_t^0, where the second term is zero since $\theta = 0$ at $z = b$, and so b^1 is known since b^0 is simply $b_\mathrm{w} = t$.

The numerical scheme (43) remains valid but now

$$\left.\frac{\partial z_\mathrm{i}}{\partial t}\right|_j = \frac{j}{J_\mathrm{i}} b_t^n, \tag{65}$$

where b_t^n is given in (64). Inside the water layer the numerical scheme is derived identically to that for the ice layer (43), namely

$$\left[r_\mathrm{w} + \frac{v_\mathrm{w}}{2}\left.\frac{\partial z_\mathrm{w}}{\partial t}\right|_{j+\frac{1}{2}}\right]\theta_{j+1}^{n+1} - \left[1 + 2r_\mathrm{w} + \frac{v_\mathrm{w}}{2}\left(\left.\frac{\partial z_\mathrm{w}}{\partial t}\right|_{j+\frac{1}{2}} - \left.\frac{\partial z_\mathrm{w}}{\partial t}\right|_{j-\frac{1}{2}}\right)\right]\theta_j^{n+1} + \left[r_\mathrm{w} - \frac{v_\mathrm{w}}{2}\left.\frac{\partial z_\mathrm{w}}{\partial t}\right|_{j-\frac{1}{2}}\right]\theta_{j-1}^{n+1} = -\theta_j^n, \tag{66}$$

Please cite this article in press as: S.L. Mitchell, T.G. Myers, Approximate solution methods for ..., Appl. Math. Comput. (2008), doi:10.1016/j.amc.2008.02.031

which holds for $j = 1, \ldots, J_w - 1$ and where

$$r_w = \frac{\Delta t}{\epsilon_w \Delta z_w^{n+1\,2}}, \quad v_w = \frac{\Delta t}{\Delta z_w^{n+1}}, \quad \Delta z_w^{n+1} = \frac{h^{n+1}}{J_w}, \quad \left.\frac{\partial z_w}{\partial t}\right|_j = \frac{j}{J_w} h_t^n. \tag{67}$$

Finally, the boundary condition (ii) at the water/air interface is similar to (46), and so

$$-\left[1 + 2r_w + 2p_w \Delta z_w^{n+1} r_w + p_w \Delta z_w^{n+1} h_t^n \frac{v_w}{2} - \frac{v_w}{2}\left.\frac{\partial z_w}{\partial t}\right|_{J_w - \frac{1}{2}}\right]\theta_{J_w}^{n+1} + \left[2r_w - \frac{v_w}{2}\left.\frac{\partial z_w}{\partial t}\right|_{J_w - \frac{1}{2}}\right]\theta_{J_w - 1}^{n+1}$$
$$= -\theta_{J_w}^n - 2(P_w - p_w)\Delta z_w^{n+1} r_w - (P_w - p_w)\Delta z_w^{n+1} h_t^n \frac{v_w}{2}, \tag{68}$$

with (i) again found from setting $p_w = 0$.

6. Results

6.1. Rime results

Table 1 shows standard physical parameter values for ice and water, applicable to aircraft icing conditions, taken from [1]. We begin with the case of the fixed energy boundary condition (22i). As discussed above, both the perturbation and HBI solutions in fact equal the exact solution in this case, and we therefore use this case to test the validity of the numerical scheme. The end of the rime phase is $t_w = 1/P_i = 0.893533$ which is independent of ΔT. Table 2 gives the numerical predictions of t_w as we reduce the mesh size (i.e. we double m where $\Delta t = 1 \times 10^{-4}/m$ and $J_i = 40 \times m$) for two values of ΔT. Observe that both columns converge to the exact t_w. As discussed in Section 6.1 we only consider $\Delta T \in [1, 5.5]$ since this is the range of validity for the perturbation solution in the glaze phase. However, in the rime phase the restriction is $\Delta T < Q_i/q_l \approx 18.89$, which is needed to ensure that there is a positive gradient in the variable energy condition (ii), as discussed at the end of Section 5.1. Although not shown in Table 2, choosing larger values of ΔT in the numerical solution also shows the same predictions. When $m = 16$ we find agreement with the exact solution to 4 d.p. and so we use $m = 16$ in numerical calculations from now on.

The results for the variable energy boundary condition (22ii) are of more interest since t_w now changes as ΔT varies. In Table 3 we present values of ϵ_i, H, P_i and p_i for $\Delta T = 5{,}2$. We refer to the perturbation solutions $T = T_0$, $T = T_0 + \epsilon_i T_1$ and $T = T_0 + \epsilon_i T_1 + \epsilon_i^2 T_2$ as "Pert0", "Pert1" and "Pert2", respectively (after convert-

Table 1
Physical parameter values for ice and water for aircraft icing conditions [1]

c_i	2050 J/kg K	c_w	4218 J/kg K
k_i	2.18 W/m K	k_w	0.57 W/m K
ρ_i	917 kg/m^3	ρ_w	1000 kg/m^3
L_f	3.34×10^5 J/kg	$\dot{m}$	0.05 kg/m^2 s
Q_i	1.869×10^4 J/m^2 s	Q_w	1990 J/m^2 s
q_l	989.3 W/m^2 K	q_m	956.9 W/m^2 K
$\widehat{T}_f$	273 K		

Table 2
Numerical prediction of t_w for $\Delta T = 5$ and $\Delta T = 2$

Mesh size	$\Delta T = 5$	$\Delta T = 2$
$m = 1$	$t_w = 0.8932000$	$t_w = 0.8934000$
$m = 2$	$t_w = 0.8933500$	$t_w = 0.8934500$
$m = 4$	$t_w = 0.8934500$	$t_w = 0.8935000$
$m = 8$	$t_w = 0.8934875$	$t_w = 0.8935125$
$m = 16$	$t_w = 0.8935125$	$t_w = 0.8935250$

The numerical time-step is $\Delta t = 1 \times 10^{-4}/m$ and mesh spacing is $J_i = 40 \times m$.

Please cite this article in press as: S.L. Mitchell, T.G. Myers, Approximate solution methods for ..., Appl. Math. Comput. (2008), doi:10.1016/j.amc.2008.02.031

Table 3
Scaling parameters in the rime period for various ΔT

	ϵ_i	H	P_i	p_i
$\Delta T = 5$	0.03069	0.0006527	1.1191528	0.29620
$\Delta T = 2$	0.01228	0.0002611	1.1191528	0.11848

ing back from $S(y, b)$ to $T(z, t)$). For $\Delta T = 5$ the numerical solution gives $t_w = 1.211219$ whilst the predictions for the approximate solutions (and the differences from the numerical solution) are: $t_w = 1.215137$ (0.32%), $t_w = 1.211171$ (0.0040%), $t_w = 1.211258$ (0.0032%) and $t_w = 1.21221$ (0.082%) for the Pert0, Pert1, Pert2 and HBI solutions, respectively. We can also look at the errors between the temperatures T for the various approximate solutions. If we define $E_- = |T_{num} - T_-|$ and calculate the L_2 norm $L_{2,-} = \|E_-\|_2 = \left(\sum E_-^2\right)^{1/2}$ then $L_{2,pert0} = 1.566 \times 10^{-2}$, $L_{2,pert1} = 4.78 \times 10^{-4}$, $L_{2,pert2} = 1.838 \times 10^{-4}$ and $L_{2,hbim} = 2.192 \times 10^{-3}$. Using smaller values of ΔT gives slightly smaller times to melting t_w, i.e. $t_w \approx 0.9989$ for $\Delta T = 2$. However, the resulting errors all show the same trend as for $\Delta T = 5$, and in particular that Pert2 is the most accurate solution.

6.2. Glaze results

Typical solutions for the temperatures and ice heights b are shown in Figs. 3 and 4, respectively, for both cases p_i, $p_w = 0$ and p_i, $p_w \neq 0$, with $\Delta T = 5$. Table 4 shows the L_2 errors between each of the approximate solutions, Pert0, Pert1, Pert2 and HBI, and the numerical solution. In both cases, the L_2 errors for temperature in the ice, T, show that Pert2 is significantly more accurate than the other approximations. The HBI solution is better than both Pert0 and Pert1 which is also true for the errors in the ice height b. However, for the errors in the water layer θ, the HBI solution is very inaccurate for boundary condition (i) but much better for boundary condition (ii). The errors for T for Pert0 and Pert1 are identical which is due to the fact that both of these expansions use $T = T_0$ (i.e. $S = S_0$) because the next order corrections are $\mathcal{O}(\epsilon_w^2)$. The high errors in b are due to the fact that the glaze calculation starts at a different t_w for each solution.

The errors in Table 4 and the profiles in Figs. 3 and 4 seem to indicate that it is acceptable to use the HBI solution in the ice layer but the perturbation solution (up to second-order accuracy) must be used in the water layer. This will avoid some of the lengthy calculations required for the perturbation expansion. In [19] a similar approximate solution was determined for the one-dimensional melting of a finite thickness layer. A perturbation expansion was used in the thin liquid layer and an HBI solution used in the solid thicker layer.

Eq. (55) only involves first-order derivatives of b. If we use t as the time variable, the second-order term in the corresponding version of (55) involves b_{tt} and b_t^2 so we end up with a second-order equation, with a small

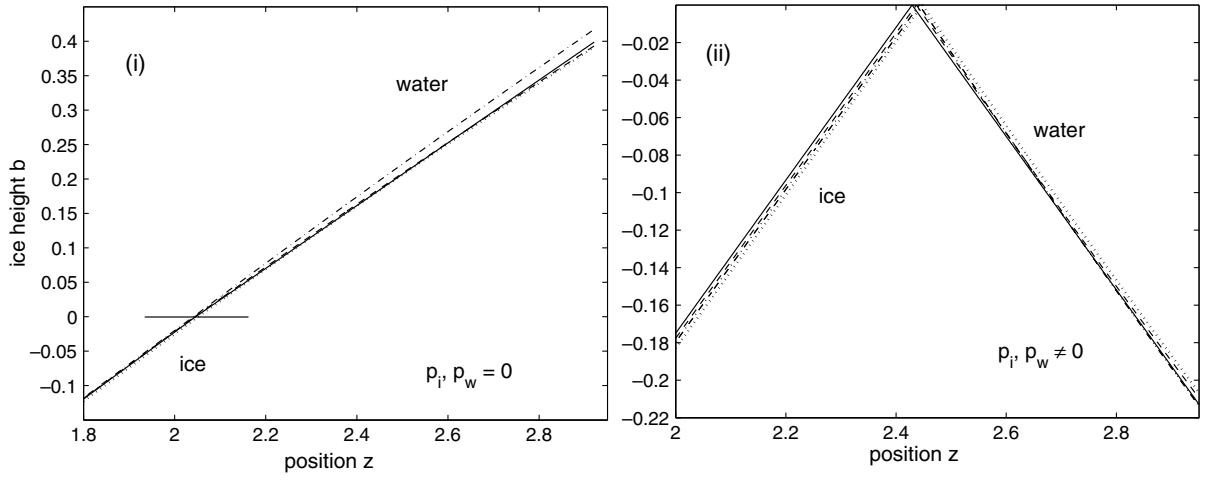

Fig. 3. Plots of the temperatures T and θ for glaze growth for the two boundary conditions (19) with $\Delta T = 5$. Shown are the numerical solution (solid line), Pert1 (dotted line), Pert2 (dashed line) and HBI (dot-dashed line).

Please cite this article in press as: S.L. Mitchell, T.G. Myers, Approximate solution methods for ..., Appl. Math. Comput. (2008), doi:10.1016/j.amc.2008.02.031

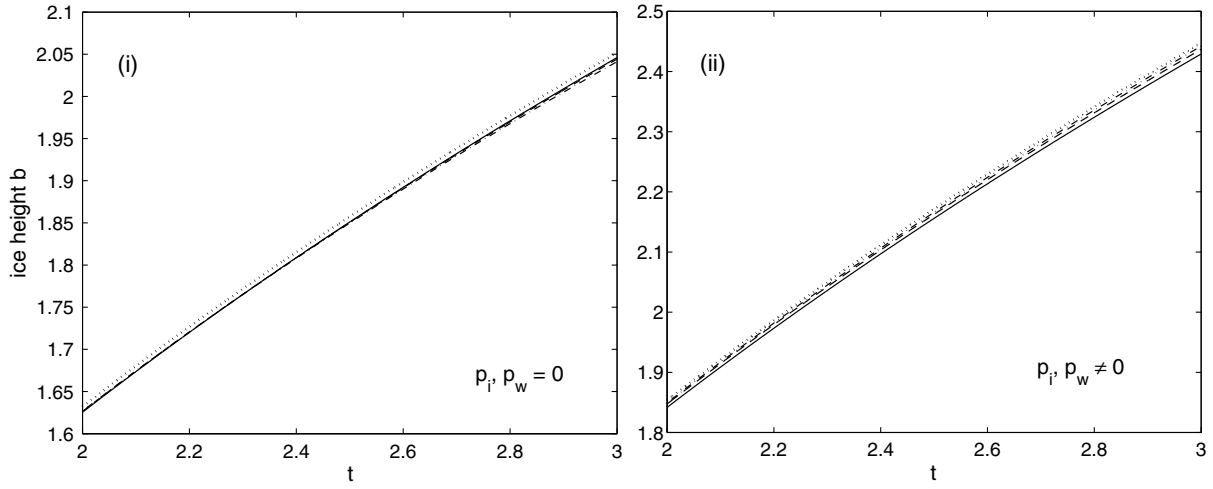

Fig. 4. Plots of ice height b for glaze growth for the two boundary conditions (19) with $\Delta T = 5$. Shown are the numerical solution (solid line), Pert1 (dotted line), Pert2 (dashed line) and HBI (dot-dashed line).

Table 4
Table showing the L_2 errors for T, θ and b (between each approximate solution and the numerical solution) from Figs. 3 and 4 in the glaze period

Error	$p_i = 0$, $p_w = 0$				$p_i \neq 0$, $p_w \neq 0$			
	Pert0	Pert1	Pert2	HBI	Pert0	Pert1	Pert2	HBI
T	$1.90e^{-2}$	$1.90e^{-2}$	$9.02e^{-5}$	$2.42e^{-3}$	$3.17e^{-2}$	$3.17e^{-2}$	$1.70e^{-4}$	$3.91e^{-3}$
θ	$4.32e^{-2}$	$4.45e^{-2}$	$3.69e^{-2}$	$2.33e^{-1}$	$5.06e^{-2}$	$4.30e^{-2}$	$2.05e^{-2}$	$3.59e^{-2}$
b	0.350	0.283	0.097	0.128	0.578	0.592	0.292	0.422

parameter in front of the leading order term. We also only have a single initial condition on b. Carrying on to higher order terms then introduces higher order derivatives. Using $t = t(b)$ results in a first-order equation, and this is the reason for making this transformation.

Lower temperature ranges generally involve one more calculation. For example if we look at $\Delta T \in [5.5, 8.5]$ and set $\epsilon_i = \beta\epsilon_i^3$ then

$$S = S_0 + \epsilon_w^3 S_3 + \cdots,$$
$$\phi = \phi_0 + \epsilon_w \phi_1 + \epsilon_w^2 \phi_2 + \epsilon_w^3 \phi_3 + \cdots.$$

We find $S_3 = S_2$ from the solution above, the ϕ terms remain the same and we are left to calculate ϕ_3.

7. Conclusion

In this paper we have investigated two approximate solution methods to describe one-dimensional solidification due to incoming supercooled liquid impacting on a fixed temperature substrate, which is kept below the melting temperature. Firstly, we applied a perturbation expansion to the non-dimensional system. Using the boundary immobilisation method allowed us to carry out the expansion to second-order, making it more accurate than in previous investigations. The use of the solid thickness as the time variable ensures that the governing ODEs are first-order and linear. Secondly, we used an alternative approximate solution, known as the heat balance integral method which is a popular technique for solving one-dimensional heat conduction problems involving a change of phase. We have also described a numerical scheme which solves the full Stefan system, and this was used to test the accuracy of the approximate perturbation and HBI solutions.

We showed that the second-order perturbation solution gave the most accurate predictions for both the temperature and height of the solid (and consequently liquid) layer. However, the perturbation solution is ana-

Please cite this article in press as: S.L. Mitchell, T.G. Myers, Approximate solution methods for ..., Appl. Math. Comput. (2008), doi:10.1016/j.amc.2008.02.031

lytically more involved since the second-order correction must be included to ensure the best accuracy, and this requires the use of the boundary immobilisation method and a change in time variable. In addition, extra complications arise with ϵ_i and ϵ_w changing orders depending on the size of ΔT. The HBI method is much easier to implement, though from examining the results in Section 7 it is clear that it is not accurate in the water layer. Therefore, it seems that the best compromise between simplicity and accuracy is to use a perturbation solution in the liquid layer and the HBI solution in the solid layer.

Acknowledgements

T.M. acknowledges the support of the National Research Foundation of South Africa, under Grant Number 2053289 as well as the Department of Mathematical Sciences at the Korean Advanced Institute of Science and Technology (KAIST) where a large part of this work was carried out. SM acknowledges the University of Cape Town Post-Doctoral Fellowship and KAIST.

Appendix. Glaze solution for the variable energy boundary condition

In Section 6.1 we determined the perturbation solutions for both the temperatures in the water and ice layers, given by T and θ, respectively, (or S and ϕ after the transformation $y = z - b(t)$ and $t = t(b)$). We wrote down results for the simpler fixed energy boundary condition (i) and here we give the results for condition (ii). These are far more complicated, especially the second-order correction ϕ_2, but this term is shown to be necessary to give a more accurate approximate solution than the HBI solution, as discussed in the results section in Section 7.

The leading order solutions corresponding to (50) are

$$S_0 = A_0(b)y, \quad A_0(b) = \frac{1}{b}, \quad \text{and} \quad \phi_0 = B_0(h)y, \quad B_0(h) = \frac{P_w - p_w}{1 + p_w h}, \tag{69}$$

with the $\mathcal{O}(\epsilon_w)$ solution given by

$$\phi_1 = B_1(b,h)y - \frac{\lambda}{2}B_0(h)y^2 + \frac{\lambda}{6}B_0'(h)h_b y^3, \tag{70}$$

where

$$B_1(b,h) = \frac{\lambda}{2}B_0(h)h\frac{2 + p_w h}{1 + p_w h} - \frac{\lambda}{6}B_0'(h)h_b h^2\frac{3 + p_w h}{1 + p_w h}, \tag{71}$$

and

$$\lambda \equiv \lambda(b,h) = \left[\frac{\partial S_0}{\partial y} - k\frac{\partial \phi_0}{\partial y}\right]_{y=0} = A_0(b) - kB_0(h) = \frac{1}{b} - \frac{k(P_w - p_w)}{1 + p_w h}. \tag{72}$$

Note that the expression in (70) involves h_b and so we will have h_{bb} terms in ϕ_2. The second-order solution S_2 is identical to that in (53) but with λ replaced by (72). However, ϕ_2 is now

$$\begin{aligned}\phi_2 = {} & B_2(b,h)y + \frac{1}{2}B_1(b,h)(kB_0(h) - \lambda)y^2 + \frac{1}{6}[\lambda(B_{1b} + B_0\lambda) - kB_1(b,h)B_0'(h)h_b]y^3 - \frac{\lambda}{24}[\lambda_b B_0(h) \\ & + 2\lambda B_0'(h)h_b]y^4 + \frac{\lambda}{120}[\lambda_b B_0'(h)h_b + \lambda(B_0''(h)h_b^2 + B_0'(h)h_{bb})]y^5,\end{aligned} \tag{73}$$

where

$$\begin{aligned}B_2(h) = {} & -\frac{1}{2}B_1(b,h)(kB_0(h) - \lambda)h\frac{2 + p_w h}{1 + p_w h} - \frac{1}{6}[\lambda(B_{1b} + B_0\lambda) - kB_1(b,h)B_0'(h)h_b]h^2\frac{3 + p_w h}{1 + p_w h} + \frac{\lambda}{24} \\ & \times [\lambda_b B_0(h) + 2\lambda B_0'(h)h_b]h^3\frac{4 + p_w h}{1 + p_w h} - \frac{\lambda}{120}[\lambda_b B_0'(h)h_b + \lambda(B_0''(h)h_b^2 + B_0'(h)h_{bb})]h^4\frac{5 + p_w h}{1 + p_w h}.\end{aligned} \tag{74}$$

The Stefan condition is again given by (55) and so b can be determined using the initial condition $b(t_w) = t_w$. Note that the expressions for ϕ_1 and ϕ_2 both involve h_b and the expression for ϕ_2 also involves h_{bb}. Hence we must determine h_b to first-order and h_{bb} to leading order. As discussed in Section 7, $h_b = (t_b - 1)/\rho$. Since $t_b = \left(\frac{db}{dt}\right)^{-1}$ we use (55) to give

$$t_b = \{A_0(b) - kB_0(h) - \epsilon_w kB_1(b,h)\}^{-1}. \tag{75}$$

However, $B_1(b, h)$ also involves h_b and so we write $t_b = t_{b,0} + \epsilon_w t_{b,1}$. After substitution of expressions for $A_0(b)$, $B_0(h)$ and $B_1(b, h)$ into (75) we find that

$$t_{b,0} = \frac{1}{\lambda}, \quad t_{b,1} = \frac{1}{\lambda}\left\{\frac{k}{2}B_0(h)h\frac{2+p_w h}{1+p_w h} - \frac{k}{6\rho}B_0'(h)(t_{b,0}-1)h^2\frac{3+p_w h}{1+p_w h}\right\}.$$

Also, to leading order in ϵ_w it can easily be shown that

$$t_{bb} = -\frac{1}{(A_0(b) - KB_0(h))^2}\left[A_0'(b) - \frac{k}{\rho}B_0'(h)\left(\frac{1}{(A_0(b) - KB_0(h))^2} - 1\right)\right].$$

References

[1] T.W. Brakel, J.P.F. Charpin, T.G. Myers, One dimensional ice growth due to incoming supercooled droplets impacting on a thin conducting substrate, Int. J. Heat Mass Transfer 50 (2007) 1705–2694.
[2] J. Caldwell, Y.Y. Kwan, Perturbation methods for the Stefan problem with time-dependent boundary conditions, Int. J. Heat Mass Transfer 46 (2003) 1497–1501.
[3] J. Crank, Two methods for the numerical solution of moving boundary problems in diffusion and heat flow, Quart. J. Mech. Appl. Math. 10 (2) (1957) 220–231.
[4] A.C. Fowler, Mathematical Models in the Applied Sciences, Cambridge University Press, 1997.
[5] I.A. Frigaard, Solidification of spray formed billets, J. Eng. Math. 31 (1997) 411–437.
[6] R.W. Gent, N.P. Dart, J.T. Cansdale, Aircraft icing, Phil. Trans. R. Soc. Lond. A 358 (2000) 2873–2911.
[7] T.R. Goodman, The heat-balance integral and its application to problems involving a change of phase, Trans. ASME 80 (1958) 335–342.
[8] T.R. Goodman, J.J. Shea, The melting of finite slabs, J. Appl. Mech. 27 (1960) 16–27.
[9] E. Gutierrez-Miravete, E.J. Lavernia, G.M. Trapaga, J. Szekely, N.J. Grant, Mathematical model of the spray deposition process, Metall. Trans. A 20 (A) (1989) 71–85.
[10] C.L. Huang, Y.P. Shih, Perturbation solutions of planar diffusion-controlled moving-boundary problems, Int. J. Heat Mass Transfer 18 (1975) 689–695.
[11] S. Kutluay, A.R. Bahadir, A. Ozdes, The numerical solution of one-phase classical Stefan problem, J. Comp. Appl. Math. 81 (1997) 135–144.
[12] L. Makkonen, Models for the growth of rime, glaze icicles and wet snow on structures, Phil. Trans. R. Soc. Lond. A 358 (2000) 2913–2939.
[13] L. Makkonen, M. Auttti, Wind Energy-technology and Implementation, The Effects of Icing on Wind Turbines, Elsevier Science Publishing, 1991.
[14] T.G. Myers, An extension to the Messinger model for aircraft icing, AIAA J. 39 (2) (2001).
[15] T.G. Myers, J.P.F. Charpin, A mathematical model for atmospheric ice accretion and water flow on a cold surface, Int. J. Heat Mass Transfer 47 (2007) 5483–5500.
[16] T.G. Myers, J.P.F. Charpin, S.J. Chapman, The flow and solidification of a thin fluid film on an arbitrary three-dimensional surface, Phys. Fluids 14 (8) (2002) 2788–2803.
[17] T.G. Myers, J.P.F. Charpin, C.P. Thompson, Slowly accreting ice due to supercooled water impacting on a cold surface, Phys. Fluids 14 (1) (2002) 240–256.
[18] T.G. Myers, D.W. Hammond, Ice and water film growth from incoming supercooled droplets, Int. J. Heat Mass Transfer 42 (1999) 2233–2242.
[19] T.G. Myers, S.L. Mitchell, G. Muchatibaya, M.Y. Myers, A cubic heat balance integral method for one-dimensional melting of a finite thickness layer, Int. J. Heat Mass Transfer 50 (2007) 5305–5317.
[20] G.I. Poots, Ice and Snow Accretion on Structures, Research Studies Press, 1996.
[21] S.K. Thomas, R.P. Cassoni, C.D. MacArthur, Aircraft anti-icing and de-icing techniques and modelling, J. Aircraft 33 (5) (1996) 841–854.

Please cite this article in press as: S.L. Mitchell, T.G. Myers, Approximate solution methods for ..., Appl. Math. Comput. (2008), doi:10.1016/j.amc.2008.02.031